Desalination and Water Treatment
www.deswater.com

doi: 10.1080/19443994.2013.839404

53 (2015) 99–108
January

Taylor & Francis
Taylor & Francis Group

Mahogany fruit shell: a new low-cost adsorbent for removal of methylene blue dye from aqueous solutions

Ashish S. Sartape[a], Suryakant A. Patil[b], Sandip K. Patil[b], Suresh T. Salunkhe[a], Sanjay S. Kolekar[b,*]

[a]*Department of Chemistry, Balwant College, Vita, Dist. Sangli 415 311, India*
[b]*Department of Chemistry, Shivaji University, Kolhapur 416 004, India*
Tel. +91 9881762426; email: kolekarss2003@yahoo.co.in

Received 20 June 2013; Accepted 9 August 2013

ABSTRACT

In the present study, we have introduced a new effective and economical adsorbent, Mahogany fruit shell. This adsorbent has porous nature and essential active groups are present on their surfaces which enhance its capability of adsorption. Developed adsorbent was characterized with Fourier transform infrared spectroscopy, scanning electron microscopy, etc. techniques which also support to confirm successful adsorption. In the present study, batch adsorption experiments were carried out as a function of pH, contact period, dye concentration, adsorbent dosage, etc. for maximum removal of methylene blue, a basic dye from aqueous solution. Mahogany fruit shell adsorbent had succeeded to remove basic dye up to 99.05% at pH 9. The experimental data are fitted well to the Langmuir adsorption isotherm. Thermodynamic parameters such as (ΔG°), (ΔH°), and (ΔS°) were calculated, which indicated that the adsorption is spontaneous and endothermic in nature. The Mahogany fruit shell had showed great adsorption capacity to remove the methylene blue.

Keywords: Adsorption; Mahogany fruit shell; Kinetic; Isotherm; FTIR study

1. Introduction

For decades, water pollution management has been prime area of scientific concern. With the development of technology and industry, more and more attention has been paid to water pollution which contains dyes [1]. Considerable quantity of water and chemicals are utilized in textile industries for wet processing of textiles at every step such as desizing, scouring, bleaching, dyeing, printing, and finishing [2]. Dye wastewater arises as a direct result of the production of the dye, and also as a consequence of its use in the textile and other industries. There are more than 1,00,000 commercially available dyes and nearly 7×10^5 tones of dyes produced annually. It is estimated that 2% of dyes produced annually are discharged in effluent from manufacturing operations while 10% is discharged from textile and associated industries [3].

The dyes are highly hazardous to aquatic systems, due to their carcinogenic, mutagenic, toxic, and allergic nature. The difficulty of biodegradation of the dyes is related to their synthetic origin and stable complex aromatic structures [4]. Methylene blue (MB) can cause eye burns which may be responsible for

*Corresponding author.

permanent injury to the eyes of human and animals. On inhalation, it can give rise to short periods of rapid or difficult breathing while ingestion through mouth produces a burning sensation and may cause nausea, vomiting, profuse sweating, mental confusion, and methemoglobinemia [5]. MB exhibits several synergistic modes of actions which enable the dose-limiting neurotoxicity of alkylating chemotherapy with ifosfamide in cancer patients to be overcome [6]. Therefore, the treatment of effluent containing such dye is of interest due to its harmful impacts on receiving waters.

In recent years, processes such as electrochemical, membrane filtration, biosorption, ion-exchange, photocatalytic degradation, coagulation/flocculation, electrocoagulation, ozonation, etc. have been applied. But it is found that either the method is expensive or do not eradicate the dye completely. The treatment by electrochemical or photochemical methods also poses problems of generation of some toxic by-products or intermediates [7]. The hunt for a safe, economic, fast, and most suitable water treatment process finally concluded at adsorption technique and for the last two decades this technique has established as the most powerful tool in the water treatment technology.

This study introduces the novel adsorbent Mahogany fruit shell (MFS) for removing MB. Mahogany is having several medicinal uses and very popular for its wood, as it has been used for preparing number of stuffs. But its fruit shell is unemployed, so it was structured as adsorbent to remove MB from aqueous solutions. The optimum conditions like pH, agitation period, agitation speed, initial concentration of MB, etc. were investigated for maximum removal of MB. The study was extended with applying isotherm and kinetic well-known models. The results of this study divulge that, the present adsorbent is effective and economical for removal of MB dye from aqueous solution.

2. Experimental

2.1. Preparation of materials

Swietenia mahagoni, known as West Indian or Indian Mahogany, belongs to Meliaceae family. The MFS has been employed successfully as adsorbent in this study without any chemical or physical treatment. The fruit shells were dried naturally. It was washed thoroughly under tap water to remove dirt and again dried in oven at 383 K for 24 h, and then cut into small pieces and again washed. The dried sample was crushed and at this stage the material was washed till all coloring contents are removed out which may interfere into further process. The material was dried at 383 K for 24 h and sieved through BSS 25. The MB dye stock solution of 1 g/dm^3 was prepared with deionized water. All chemicals used in this study were of analytical reagent grade and purchased from S. D. Fine Chem. Ltd, India.

2.2. Batch adsorption experiment

The experiments were carried out by batch adsorption method. The isotherm study has been done by varying the initial concentration of the MB from 100 to 700 mg/dm^3 at constant MFS of 450 mg as adsorbent. The batch was agitated for 420 min on orbital shaker at constant temperature 299 ± 2 K and at pH of 9 in the Erlenmeyer flasks with 180 rpm as agitation speed. For the thermodynamic study, temperature was varied from 303 to 323 K. The equilibrium adsorption capacity of MFS was evaluated.

3. Results and discussion

3.1. Characterization of adsorbent

The characterization of MFS has been done with Fourier transform infrared spectroscopy (FTIR), scanning electron microscopy (SEM) and C, H, N, S analyzer. Various properties such as ash content, bulk density, and moisture content were also determined which was observed as 2.53%, 0.237 gm/cm^3, and 9.92%, respectively.

The FTIR (Perkin–Elmer Spectrum 100) spectrum of MFS is given in Fig. 1. In the spectrum (Fig. 1), the value at 3,400 cm^{-1} has denoted the presence of OH group, while 2,923 cm^{-1} corresponds to C–H stretching. The values at 1,733, 1,626, 1,434, 1,372, 1,250, and

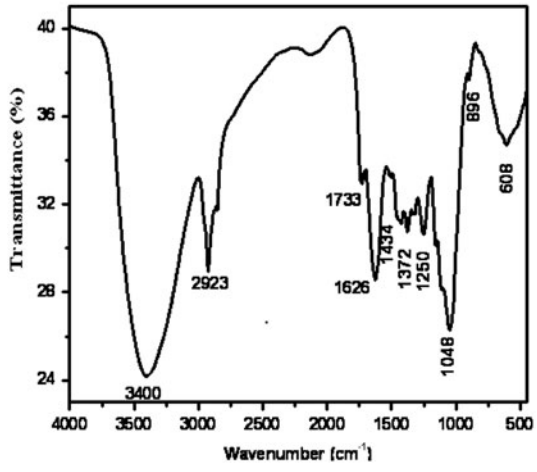

Fig. 1. FTIR spectrum of MFS.

1,049, 896 cm^{-1} give the information about the presence of C=O, N–H bending, $–CH_2$ from cellulose, N=O symmetric stretching, C–O stretch, and C–H bending and =C–H bending, respectively. The SEM (JEOL, JSM-6360) images are shown in Fig. 3(A) before adsorption and Fig. 3(B) after adsorption. The C, H, N, S elemental analyzer (Quanta 3D FEI) confirms that the presence of carbon is maximum amongst all as 60.77% along with hydrogen and nitrogen 1.76 and 0.57%.

3.2. Analysis of adsorption of MB on MFS

The adsorption of MB on MFS was clearly identified from Fig. 2, FTIR spectrum of MFS (Fig. 2(A)), MB (Fig. 2(B)), and MB adsorbed on MFS (Fig. 2(C)). The major peaks are present from 2000 to 400 cm^{-1}. The several peaks from MFS and MB are merged or they are slightly shifted. The peak at 1,736 cm^{-1} in Fig. 2(C) is due to C=O which is only present in MFS (Fig. 2(A)) at 1,733 cm^{-1}. The peak at 1,626 cm^{-1} is due to presence of N–H bending present in MFS (Fig. 2(A)) and 1,601 cm^{-1} peak from (Fig. 2(B)) MB is due to C=C group. Both these are merged and show weak peak at the 1,620 and 1,602 cm^{-1} and form broad peak together. The peak at 1,508 cm^{-1} is due to C=N stretching from MB in Fig. 2(C) as it shows peak originally at 1,488 cm^{-1} in MB (Fig. 2(A)). Peak at 1,383 cm^{-1} in Fig. 2(C) is due to merging of peak from both MFS and MB peak at 1,372 and 1,396 cm^{-1}, respectively but peak at 1,330 cm^{-1} (Fig. 2(C)) is shifted from 1,356 cm^{-1} which indicates C–H bending in MB (Fig. 2(B)). In case of MFS, peak at 1,250 cm^{-1} (Fig. 2(A)) is due to C–O stretching which is shifted to 1,248 cm^{-1} in Fig. 2(C) MB adsorbed on MFS. The peaks from MB (Fig. 2(B)) at 1,142 and 1,182 cm^{-1} are due to merging of C=S stretching with strong peak at 1,048 cm^{-1} from MFS (Fig. 2(A)), and show broad peak at 1,051 cm^{-1} in MB adsorbed on MFS (Fig. 2 (C)). Peak at 886 cm^{-1} in MB (Fig. 2(B)) is due to C=C aromatic bending, it slightly shifted at 889 cm^{-1} in Fig. 2(C). The FTIR results reveal the adsorption of MB on MFS. The merging and shifting was already observed in some reports [8].

In SEM study, the change in surface morphology was observed. In Fig. 3(A) before adsorption and Fig. 3(B) after adsorption, it is clearly observed that the layer of adsorbed dye was formed on surface. Before adsorption, the MFS surface was very rough and after adsorption of MB dye appears like formation of a smooth layer on it. The rough surface is made from incorporation of various small particles of MFS adsorbent, as the particles are smaller in size

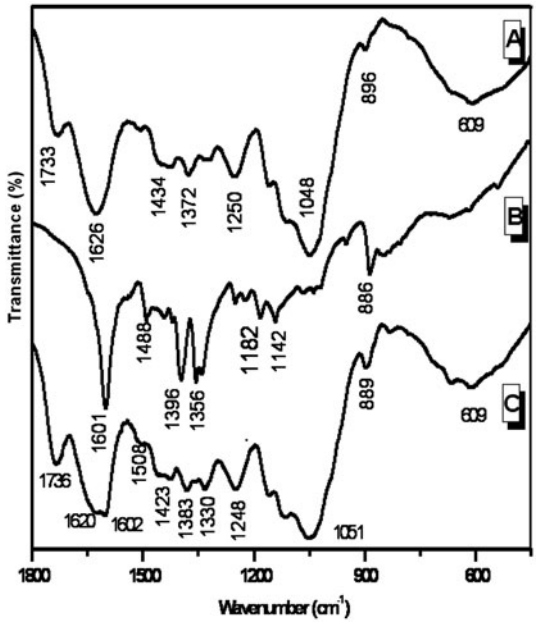

Fig. 2. FTIR spectrum of (A) MFS, (B) MB, and (C) MB adsorbed on MFS.

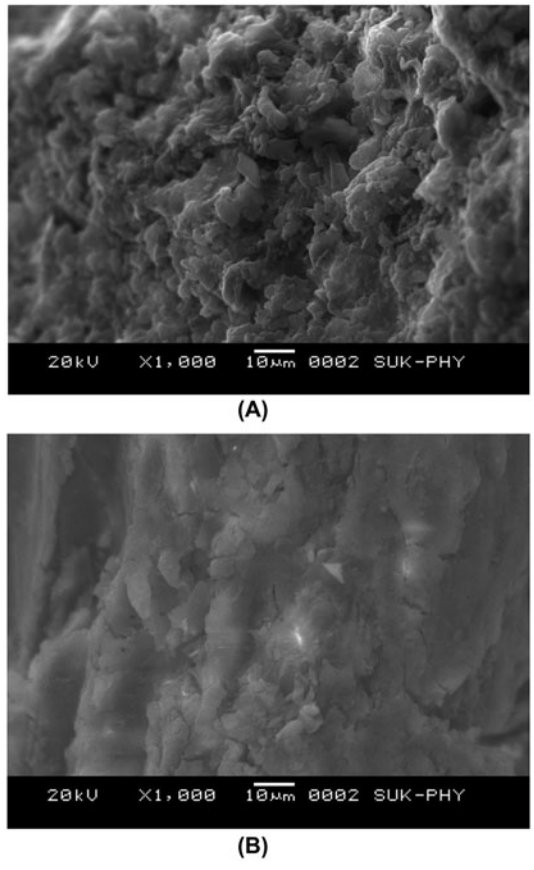

Fig. 3. (A) SEM image before adsorption of MB and (B) SEM image before adsorption of MB.

results in larger the surface area which is favorable to greater the adsorption. Similar observations in case of SEM are also reported [9].

3.3. Effect of pH and determination of pH_{ZPC}

The pH study is important for development of every successful method. In the present study, pH was varied from 1 to 11 with 100 mg/dm^{3}MB concentration, 450 mg MFS, 299 ± 2 K temperature, and agitated at 180 rpm for 420 min. The maximum adsorption was observed above pH 6 (Fig. 4). At pH 6, the MB removal percentage was 98.24% and amount adsorbed was 10.91 mg/g which was increased up to 99.05% and 11.01 mg/g when pH increases up to 9.0 (Fig. 4). As the maximum removal was observed at pH 9.0, it was kept constant pH throughout the study.

The MB adsorption usually increases as the pH is increased. Lower adsorption of MB at acidic pH is probably due to the presence of excess H^+ ions competing with the cation groups on the dye for adsorption sites. At higher pH, the surface of MFS particles may get negatively charged, which enhances the adsorption of positively charged dye cations through electrostatic forces of attraction [10]. The present observations are in good agreement with the previous findings by Cengiz [11].

The determination of point of zero charge (pH_{ZPC}) of MFS was performed according to the solid addition method [9]. The pH_{ZPC} of an adsorbent is a very important characteristic feature that determines the pH at which the adsorbent surface has net electrical neutrality. At this value, the acidic or basic functional groups no longer contribute to the pH of the solution. The value of pH_{ZPC} observed for this study was 6.44.

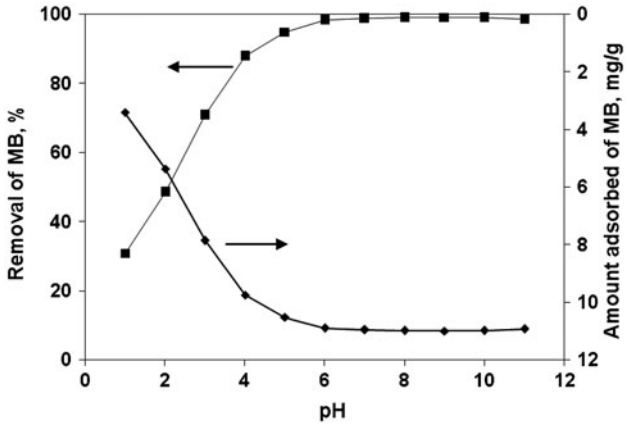

Fig. 4. Effect of pH on removal, % and amount of MB adsorbed, mg/g MB = 100 mg/dm^3, time = 420 min, T = 299 ± 2 K, MFS = 450 mg, agitation speed = 180 rpm.

When solution pH > pH_{ZPC}, the surface of the adsorbent gets more negatively charged by loosing protons and therefore favors uptake of cationic dyes due to increased electrostatic force of attraction [12]. Thus, MB adsorption onto MFS was favored at solution pH higher than 6.44 (pH_{ZPC}).

3.4. Effect of time

The effect of agitation period on the removal of MB by MFS was studied with MB 100 mg/dm^3 at pH 9. The agitation period was varied from 0 to 600 min at constant temperature. The removal of adsorbate is rapid in early stages but it gradually slows down until it reaches the equilibrium. After completion of 120 min, more than 67% removal of MB was reported while it had taken from 240 to 420 min for removal of 90 to 99.05% MB. This is due to fact that a large number of vacant surface sites are available for adsorption during the initial stage, and after a lapse of time the remaining vacant surface sites are difficult to be occupied due to repulsive forces between the solute molecules on the solid surface and in bulk phase [9]. The equilibrium was attained after shaking for 420 min. Once equilibrium was attained, the percentage sorption of MB did not change with further increases of time. So, it was assumed that longer treatment might not have further effect to change the properties of the adsorbent therefore time of 420 min was fixed for further study.

3.5. Effect of initial concentration of MB

The amount of MB adsorbed per unit mass of adsorbent increased with the increase in initial concentration and percentage removal of MB from aqueous solution decreased with the increase in initial concentration (Fig. 5). The amount of MB adsorbed at equilibrium increased from 11.01 to 50.73 mg/g as the initial concentration increased from 100 to 700 mg/dm^3. The initial concentration provides an important driving force to overcome all mass transfer resistances of the MB between the aqueous and solid phases. Hence, a higher initial concentration of dye will enhance the adsorption process [13]. The effect of initial concentration was studied at constant parameters like pH, temperature, agitation speed, time, etc.

3.6. Effect of adsorbent dosage

The effect of adsorbent dosage on the removal of MB was studied for an initial dye concentration of 100 mg/dm^3, by varying the adsorbent from 50 to 450 mg at temperature 299 ± 2 K and by keeping all

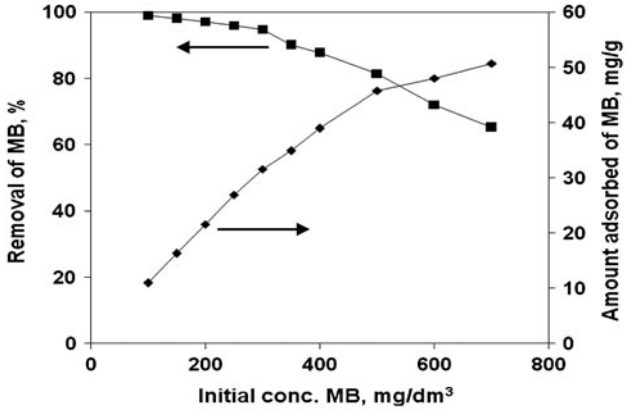

Fig. 5. Effect of concentration of MB on amount adsorbed, mg/g and removal, % of MB time = 420 min, pH = 9, $T = 299 \pm 2$ K, MFS = 450 mg, agitation speed = 180 rpm.

other parameters constant. Removal of MB dye was increased from 5% up to 99.05% with increase in adsorbent dosage. This may be due to the fact that the active sites could be effectively utilized when the dosage was low (i.e. low ratio of adsorbent/adsorbate). When the adsorbent dosage is higher (high ratio of adsorbent /adsorbate), it is more likely that a significant portion of the available active sites remains uncovered, leading to lower specific uptake [12]. The amount of dye adsorbed per unit mass of adsorbent decreased with increasing adsorbent mass, due to the reduction in effective surface area.

3.7. Effect of temperature and agitation speed

The temperature plays a vital role in the adsorption capacity of adsorbent. The temperature was increased from 303 to 323 K with 5 K interval and the results were showing very much difference in the adsorption; it was increased from 53.05 to 61.85 mg/g. This indicates that the adsorption reaction was endothermic in nature. The enhancement in the adsorption capacity may be due to the chemical interaction between adsorbate and adsorbent, creation of some new adsorption sites, and the increased rate of intraparticle diffusion of MB into the pores of the adsorbent at higher temperatures.

In the batch adsorption systems, agitation speed plays a significant role in affecting the external boundary film and the distribution of the solute in the bulk solution. The experiments were carried out by varying agitation speed from 50 to 240 rpm by keeping all other conditions constant. With increasing agitation speed, the amount adsorbed and percentage removal of MB increased simultaneously. At the 50 rpm, 50.75% removal of MB was observed, which was increased up to 99.05% with increasing speed of agitation up to 180 rpm. The influence of agitation speed was negligible after 180 rpm; both amount and percentage remains steady so that agitation speed was decided for further study.

3.8. Adsorption isotherm

Equilibrium studies that give the capacity of the adsorbent and adsorbate are described by adsorption isotherms, which is usually the ratio between the quantity adsorbed and remained in solution at equilibrium at constant temperature. Several models have been reported in the literature to describe the experimental data of adsorption isotherms. The Langmuir and Freundlich are the most frequently employed models. In this work, both models were used to describe the relationship between the amount of dye adsorbed and its equilibrium concentration.

3.9. Langmuir isotherm

The Langmuir adsorption isotherm has been successfully applied to many adsorption processes and has been the most widely used. The Langmuir equation can be stated as [14],

$$C_e/Q_e = (1/K_L q_m) + (1/q_m)C_e \quad (1)$$

where, K_L is the Langmuir equilibrium constant of adsorption (1/mg), q_m is the quantity of adsorbate required to form a single monolayer, and q_e is the amount adsorbed on unit mass of the solid when the equilibrium concentration is C_e. A plot of C_e/q_e vs. C_e (Fig. 6) indicates a straight line of slope $1/q_m$ and an intercept of $1/K_L q_m$.

A further analysis of the Langmuir equation can be made on the basis of a dimensionless equilibrium parameter, R_L [15] also known as the separation factor, given by,

$$R_L = 1/(1 + K_L C_e) \quad (2)$$

The value of R_L lies between 0 and 1 for favorable adsorption, while $R_L > 1$ represents unfavorable adsorption, and $R_L = 1$ represents linear adsorption while the adsorption process is irreversible if $R_L = 0$.

The essential characteristic of a Langmuir isotherm, related to the isotherm shape, can be expressed in terms of a dimensionless constant separation factor, also called the equilibrium parameter R_L. The adsorption of MB on MFS follows the Langmuir isotherm model for metal adsorption. The values of q_m and K_L

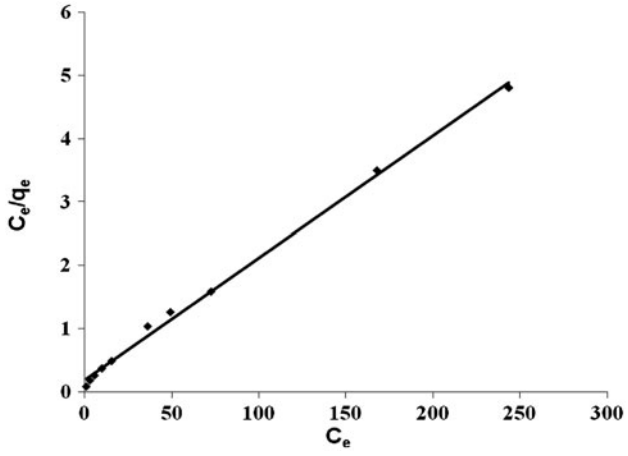

Fig. 6. Langmuir isotherm for adsorption of MB on MFS time = 420 min, pH = 9, $T = 299 \pm 2$ K, MFS = 450 mg, agitation speed = 180 rpm.

were evaluated and given in Table 1. The dimensionless parameter R_L between 0.039 and 0.913 is consistent with favorable adsorption. The high value of correlation coefficient R^2 indicates a good agreement between the parameters and confirms the monolayer adsorption of MB on the adsorbent surface.

3.10. Freundlich isotherm

The Freundlich isotherm assumes that the adsorption occurs on heterogeneous surface at sites with different energy of adsorption and with non-identical adsorption sites that are not always available. The logarithmic form of the Freundlich isotherm equation is given as [16],

$$\log q_e = \log K_f + 1/n \log C_e \quad (3)$$

where, q_e is the amount adsorbed (mg/g), C_e is the equilibrium concentration of the adsorbate (mg/L), and K_f and n are Freundlich constants related to the adsorption capacity and adsorption intensity, respectively. The Freundlich constants are given in Table 1 and from the result it may concluded that the Langmuir isotherm model fits better than the Freundlich isotherm model.

3.11. Temkin model

Temkin and Pyzhev considered the effects of indirect adsorbate–adsorbate interactions on adsorption isotherms. The heat of adsorption of all the molecules in the layer would decrease linearly with coverage due to adsorbate–adsorbate interactions [9]. The Temkin isotherm has been used in the form as follows:

$$q_e = (RT/b) \ln(K_T C_e) \quad (4)$$

It can be expressed in its linear form as,

$$q_e = B \ln(K_T + B \ln C_e) \quad (5)$$

where,

$$B = (RT/b) \quad (6)$$

The adsorption data were analyzed according to Equation (5). A plot of q_e vs. ln C_e yielded a linear line, as shown in Fig. 7 enables the determination of the isotherm constants K_T and B. K_T is the Temkin equilibrium binding constant (L/mg) corresponding to the maximum binding energy and constant B is related to heat of adsorption. The constants K_T and B together with the R^2 values are shown in Table 1. From Table 1, the Langmuir adsorption isotherm model yielded best fit as indicated by the highest R^2 values compared to the other two models.

3.12. Adsorption kinetics

The experiments were carried out at constant temperature as well as speed and pH. Amount of adsorption of MB on MFS was studied at various time intervals from 0 to 420 min. In order to investigate the mechanism of adsorption on MFS, kinetic model has been used to identify the possible mechanisms of such adsorption process. In this study, pseudo-first- and pseudo-second-order kinetic models have been proposed to elucidate the mechanism of adsorption depending on the characteristics of the adsorbent.

The following pseudo-first-order equation is used for it is simple and easy for graphical presentation [17]:

Table 1
Langmuir, Freundlich, and Temkin constant for the adsorption of MB on MFS

Langmuir constants			Freundlich constants			Temkin constants		
q_m (mg/g)	K_L (1/mg)	R^2	K_f	n	R^2	K_T (L/g)	B	R^2
51.81	0.101	0.997	12.72	3.556	0.964	2.941	7.884	0.981

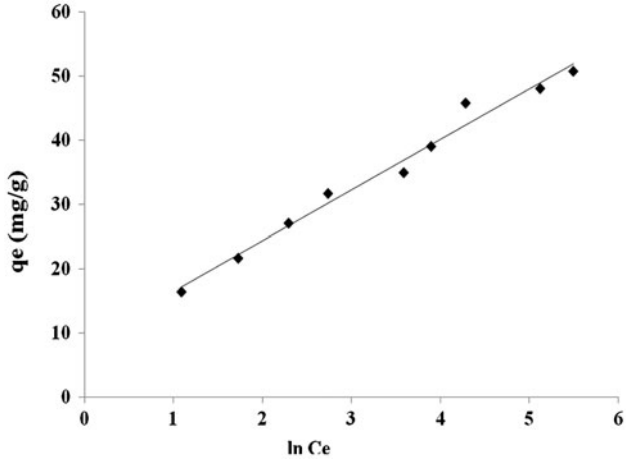

Fig. 7. Temkin isotherm for adsorption of MB on MFS time = 420 min, pH = 9, $T = 299 \pm 2$ K, MFS = 450 mg, agitation speed = 180 rpm.

$$\log (q_e - q_t) = \log q_e - k_1 t/2.303 \quad (7)$$

where q_e and q_t are the amount of solute adsorbed (mg/g) at equilibrium and at time t (min), respectively, and k_1 is the rate constant of the pseudo-first-order adsorption process. The k_1 and q_e value for the initial concentration of 100 mg/dm^3 are given in Table 2, which are not promising as compare with true value.

The corresponding pseudo-second-order rate equation [18] is,

$$t/q_t = 1/k_2 q_e^2 + t/q_e \quad (8)$$

where k_2 is the rate constant for pseudo-second-order adsorption. The pseudo-second-order rate equation is used to study the adsorption of MB on MFS. The rate parameters k_2 and q_e can be directly obtained from the intercept and slope of the plot of t/q_t vs. t (Fig. 8). The values obtained graphically for pseudo-first- and pseudo-second-order models are listed in Table 2. The results show that the pseudo-second-order model provided a better approximation to the experimental kinetic data than the pseudo-first-order model.

3.13. Intraparticle diffusion study

The adsorbate species are most probably transported from the bulk of the solution in to the solid phase through intraparticle diffusion process, which is often the rate-limiting step in many adsorption processes. The possibility of intraparticle diffusion was explored by using the intraparticle diffusion model [19].

The intraparticle diffusion varies with square root of time [20],

$$q_t = k_{id} t^{1/2} + c \quad (9)$$

where c is constant and k_{id} is the intraparticle diffusion rate constant (mg/g min$^{1/2}$), q_t is the amount adsorbed at a time (mg/g), and t is the time (min). The intraparticle diffusion rate constant (k_{id}) was determined and tabulated in Table 2.

The adsorption of MB on MFS adsorbent was a multi-step process, involving adsorption on the external surface and diffusion into the interior. All the steps slow down as the system approaches equilibrium. If the steps are independent of one another, the plot of q_t

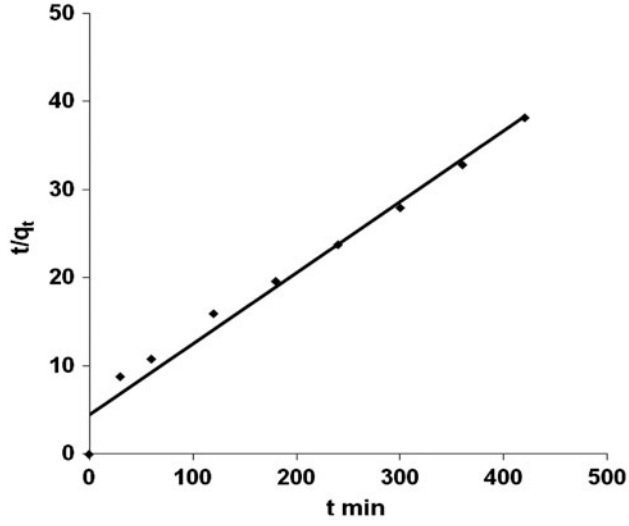

Fig. 8. Pseudo-second order plot for adsorption of MB on MFS MB = 100 mg/dm^3, pH = 9, $T = 299 \pm 2$ K, MFS = 450 mg, agitation speed = 180 rpm.

Table 2
Kinetic parameters for the adsorption of MB on MFS

Pseudo first order				Pseudo second order			Intraparticle diffusion equation	
q_e exp.(mg/g)	$k_1 \times 10^{-3}$ (min^{-1})	q_e calc. (mg/g)	R^2	$k_2 \times 10^{-3}$	q_e calc. (mg/g)	R^2	k_{id} (mg g^{-1} min^{-1})	R^2
11.01	6.40	17.02	0.932	6.26	12.64	0.991	0.512	0.942

vs. $t^{1/2}$ usually shows two or more intersecting lines depending on the exact mechanism, the first one of these lines representing surface adsorption and the second line shows intraparticle diffusion. The absence of such features in the plots of the present work indicated that the steps were indistinguishable from one another and that the intraparticle diffusion was a prominent process right from the beginning of dye-solid interaction. If the uptake of the adsorbate varies with the square root of time, intraparticle diffusion can be taken as the rate-limiting step. If the q_t vs. $t^{1/2}$ plots pass through the origin then intraparticle diffusion is the sole rate-limiting step [21]. Since this was also not the case in the present work it may be concluded that, surface adsorption and intraparticle diffusion were concurrently operating during the MB–MFS interactions.

3.14. Adsorption thermodynamics

The thermodynamic parameters such as standard Gibb's energy (ΔG°), standard enthalpy (ΔH°), and standard entropy (ΔS°) were determined at 700 mg/dm^3 MB concentration by keeping all other parameters constant

The standard Gibb's energy is given by equation,

$$\Delta G^o = -RT \ln \mathrm{Kc} \quad (10)$$

The equilibrium constant Kc was evaluated at each temperature using the following relationship. Other thermodynamic parameters such as change in standard enthalpy (ΔH°) and standard entropy (ΔS°) were determined using the equation [22],

$$\ln \mathrm{Kc} = \Delta S^o/R - \Delta H^o/RT \quad (11)$$

As the temperature increases from 303 to 323 K showed decrease in standard free energy change (ΔG°) from −3.938 to −4.611 kJ/mol. Negative values of ΔG° indicated the feasibility of the process and spontaneous nature of the adsorption with a high performance of MB for MFS. Positive value 0.746 kJ/mol of standard enthalpy change (ΔH°) indicated the endothermic nature of the process, while positive value 4.034 J/mol k of standard entropy change (ΔS°) reflected the affinity of the adsorbents for the MB.

4. Comparison of adsorption capacity of MFS with other adsorbents

The developed MFS adsorbent MB removal capacity was compared with reported adsorbents (Table 3) and it was observed that, MFS has great adsorption capacity.

Table 3
Comparison of adsorption capacity of MFS with other adsorbents

Adsorbent	q_m (mg/g)	Reference
Parthenium hysterophorus	39.68	[8]
C. racemosa var. cylindracea	5.23	[11]
Natural zeolite	16.37	[16]
Amberlite XAD-2	16.8	[18]
Neem tree	8.76	[21]
Raw kaolin	27.49	[23]
Calcined raw kaolin	13.44	[23]
Gypsum	36	[24]
Fe(III)/Cr(III) hydroxide	22.8	[25]
Polyacrylic acid-bound iron oxide magnetic nanoparticles	0.199	[26]
Multiwalled carbon nanotubes containing oxygen		
0.85%	61.10	[27]
2.16%	36.62	[27]
7.07%	25.62	[27]
Silica nanosheets	11.77	[28]
Oil palm wood activated carbon	90.9	[29]
Sunflower oil cake activated carbon	10.21	[30]
Impregnation with 0.85 H_2SO_4	16.43	[30]
Impregnation with 1.90 H_2SO_4	15.798	[30]
Straw carbon	42.60	[31]
Rice husk carbon	37.57	[31]
Groundnut shell carbon	7.50	[31]
Coconut shell carbon	8.16	[31]
Bamboo dust carbon	7.20	[31]
Activated coir pith carbon	5.87	[32]
Cotton stalk	4.52	[33]
Cotton dust	8.33	[33]
Cotton waste	9.75	[33]
Rice husk ash	18.15	[34]
Spent coffee grounds residue	18.70	[35]
Ricinus communis activated carbon	7.7	[36]
Agar	12.8	[37]
Rice husk activated carbon	9.73	[38]
Biochar wheat straw	12.03	[39]
Residue biochar	16.75	[40]
Oyster shell	0.084	[41]
Hard clam shell	0.060	[41]
Short-neck clam shell	0.893	[41]
MFS	*51.81*	*Present work*

5. Conclusions

In the present research, the adsorptive removal of MB from aqueous solution was investigated by using a MFS which is one of the most promising adsorbent

due to its low cost and easy availability. One of the essential features of this study was to use the adsorbent without any previous activation treatment which has the preparation cost nearly zero. The adsorption properties of MFS were studied, which suggests that it showed excellent adsorption capacity at pH 9. The removal of MB was possible by MFS up to 99.05% when concentration of the dye was 100 mg/dm^3. The study was evaluated with isotherm models amongst them, Langmuir adsorption was fitted better than others. The kinetic study had shown that, the pseudo-second order is more suitable than pseudo-first order. The process is endothermic and spontaneous, and evaluated thermodynamic parameters such as ΔG°, ΔH°, and ΔS° which supports the favorable adsorption. Finally, it is concluded that the MFS is inexpensive, effective adsorbent to remove MB from aqueous solutions. It is useful for wastewater treatment.

Acknowledgments

The authors acknowledge the DST-FIST, UGC-SAP facilities, Department of Chemistry, Shivaji University, Kolhapur and Balwant College, Vita, India.

References

[1] W. Wang, C. Li, J. Yao, B. Zhang, Y. Zhang, J. Liu, Rapid adsorption of neutral red from aqueous solutions by Zn3[Co(CN)6]2.nH_2O nanospheres, J. Mol. Liq. 184 (2013) 10–16.
[2] I. Haq, H.N. Bhatti, M. Asgher, Removal of solar red Ba textile dye from aqueous solution by low cost barley husk: Equilibrium, kinetic and thermodynamic study, Can. J. Chem. Eng. 89 (2011) 593–600.
[3] S.J. Allen, B. Koumanova, Decolourisation of water/wastewater using adsorption (review), J. Univ. Chem. Technol. Metall. 40 (2005) 175–192.
[4] A.N. Módenes, A.A. Ross, B.V. Souza, J. Dotto, C.Q. Geraldi, F.R.E. Quiñones, D. Kroumov, Biosorption of BF-4B reactive red dye by using leaves of macrophytes *Eichhornia crassipes*, Int. J. Bioautomation 17(1) (2013) 33–44.
[5] M. Rafatullah, O. Sulaiman, R. Hashim, A. Ahmad, Adsorption of methylene blue on low-cost adsorbents: A review, J. Hazard. Mater. 177 (2010) 70–80.
[6] A. Küpfer, C. Aeschlimann, T. Cerny, Methylene blue and the neurotoxic mechanisms of ifosfamide encephalopathy, Eur. J. Clin. Pharmacol. 50 (1996) 249–252.
[7] J. Mittal, D. Jhare, H. Vardhan, A. Mittal, Utilization of bottom ash as a low-cost sorbent for the removal and recovery of a toxic halogen containing dye eosin yellow, Desalin. Water Treat. (2013). doi: 10.1080/19443994.2013.803265.
[8] H. Lata, V.K. Garg, R.K. Gupta, Removal of a basic dye from aqueous solution by adsorption using *Parthenium hysterophorus*: An agricultural waste, Dyes Pigm. 74 (2007) 653–658.
[9] A. Ahmad, M. Rafatullah, O. Sulaiman, M.H. Ibrahim, R. Hashim, Scavenging behaviour of meranti sawdust in the removal of methylene blue from aqueous solution, J. Hazard. Mater. 170 (2009) 357–365.
[10] B.H. Hameed, D.K. Mahmoud, A.L. Ahmad, Equilibrium modeling and kinetic studies on the adsorption of basic dye by a low-cost adsorbent: Coconut (*Cocos nucifera*) bunch waste, J. Hazard. Mater. 158 (2008) 65–72.
[11] S. Cengiz, L. Cavas, Removal of methylene blue by invasive marine seaweed: *Caulerpa racemosa* var. Cylindracea, Bioresour. Technol. 99 (2008) 2357–2363.
[12] V. Ponnusami, V. Gunasekar, S.N. Srivastava, Kinetics of methylene blue removal from aqueous solution using gulmohar (*Delonix regia*) plant leaf powder: Multivariate regression analysis, J. Hazard. Mater. 169 (2009) 119–127.
[13] B.H. Hameed, Spent tea leaves: A new non-conventional and low-cost adsorbent for removal of basic dye from aqueous solutions, J. Hazard Mater. 161 (2009) 753–759.
[14] I. Langmuir, The constitution and fundamental properties of solids and liquids, J. Am. Chem. Soc. 38 (1916) 2221–2295.
[15] K.R. Hall, L.C. Eagleton, A. Acrivos, T. Vermeulen, Pore and solid diffusion kinetics in fixed bed adsorption under constant pattern conditions, Ind. Eng. Chem. Fundam. 5 (1966) 212–223.
[16] R. Han, J. Zhang, P. Han, Y. Wang, Z. Zhao, M. Tang, Study of equilibrium, kinetic and thermodynamic parameters about methylene blue adsorption onto natural zeolite, Chem. Eng. J. 145 (2009) 496–504.
[17] C. Guo, Q. Kong, J. Gao, Q. Ji, Y. Xia, Removal of methylene blue dye from simulated wastewater by alginic acid fiber as adsorbent: Equilibrium, kinetic, and thermodynamic studies, Can. J. Chem. Eng. 89 (2011) 1545–1553.
[18] F. Ferrero, Adsorption of methylene blue on magnesium silicate: Kinetics, equilibria and comparison with other adsorbents, J. Environ. Sci. 22(3) (2010) 467–473.
[19] M. Dogan, M. Alkan, A. Türkyilmaz, Y. Özdemir, Kinetics and mechanism of removal of methylene blue by adsorption onto perlite, J. Hazard. Mater. B109 (2004) 141–148.
[20] L. Xiong, Y. Yang, J. Mai, W. Sun, C. Zhang, D. Wei, Q. Chen, J. Ni, Adsorption behavior of methylene blue onto titanate nanotubes, Chem. Eng. J. 156 (2010) 313–320.
[21] K.G. Bhattacharyya, A. Sharma, Kinetics and thermodynamics of methylene blue adsorption on neem (*Azadirachta indica*) leaf powder, Dyes Pigm. 65 (2005) 51–59.
[22] Y. Yao, F. Xu, M. Chen, Z. Xu, Z. Zhu, Adsorption behavior of methylene blue on carbon nanotubes, Bioresour. Technol. 101 (2010) 3040–3046.
[23] D. Ghosh, K.G. Bhattacharyya, Adsorption of methylene blue on kaolinite, Appl. Clay Sci. 20 (2002) 295–300.
[24] M.A. Rauf, I. Shehadeh, A. Ahmed, A. AlZamly, Removal of methylene blue from aqueous solution by using gypsum as a low cost adsorbent, World Acad. Sci. Eng. Technol. 55 (2009) 608–613.
[25] C. Namasivayam, S. Sumithra, Removal of direct red 12B and methylene blue from water by adsorption onto Fe(III)/Cr(III) hydroxide, an industrial solid waste, J. Environ. Manage. 74 (2005) 207–215.
[26] S.Y. Mak, D.H. Chen, Fast adsorption of methylene blue on polyacrylic acid-bound iron oxide magnetic nanoparticles, Dyes Pigm. 61 (2004) 93–98.
[27] G.C. Chen, X.Q. Shan, Y.Q. Zhou, X. Shen, H.L. Huang, S.U. Khan, Adsorption kinetics, isotherms and thermodynamics of atrazine on surface oxidized multiwalled carbon nanotubes, J. Hazard. Mater. 169 (2009) 912–918.
[28] M. Zhao, Z. Tang, P. Liu, Removal of methylene blue from aqueous solution with silica nano-sheets derived from vermiculite, J. Hazard. Mater. 158 (2008) 43–51.
[29] A.L. Ahmad, M.M. Loh, J.A. Aziz, Preparation and characterization of activated carbon from oil palm wood and its evaluation on methylene blue adsorption, Dyes Pigm. 75 (2007) 263–272.
[30] S. Karagoz, T. Tay, S. Ucar, M. Erdem, Activated carbons from waste biomass by sulfuric acid activation and their use on methylene blue adsorption, Bioresour. Technol. 99 (2008) 6214–6222.

[31] N. Kannan, M.M. Sundaram, Kinetics and mechanism of removal of methylene blue by adsorption on various carbons: A comparative study, Dyes Pigm. 51 (2001) 25–40.
[32] D. Kavitha, C. Namasivayam, Experimental and kinetic studies on methylene blue adsorption by coir pith carbon, Bioresour. Technol. 98 (2007) 14–21.
[33] M. Ertas, B. Acemioglub, M.H. Alma, M. Usta, Removal of methylene blue from aqueous solution using cotton stalk, cotton waste and cotton dust, J. Hazard Mater. 183 (2010) 421–427.
[34] A.K. Chowdhury, A.D. Sarkar, A. Bandyopadhyay, Rice husk ash as a low cost adsorbent for the removal of methylene blue and congo red in aqueous phases, Clean-Soil, Air, Water 37 (2009) 581–591.
[35] A.S. Franca, L.S. Oliveira, M.E. Ferreira, Kinetics and equilibrium studies of methylene blue adsorption by spent coffee grounds, Desalination 249 (2009) 267–272.
[36] P. Thamilarasu, K. Karunakaran, Kinetic, equilibrium and thermodynamic studies on removal of Cr(VI) by activated carbon prepared from *Ricinus communis* seed shell, Can. J. Chem. Eng. 91 (2013) 9–18.
[37] B. Samiey, F. Ashoori, Adsorptive removal of methylene blue by agar: Effects of NaCl and ethanol, Chem. Cent. J. 6(14) (2012) 1–13.
[38] Y.C. Sharma, Uma, S. N. Upadhyay, An economically viable removal of methylene blue by adsorption on activated carbon prepared from rice husk, Can. J. Chem. Eng. 89(2) (2011) 377–383.
[39] Y. Liu, X. Zhao, J. Li, D. Ma, R. Han, Characterization of biochar from pyrolysis of wheat straw and its evaluation on methylene blue adsorption, Desalin. Water Treat. 46(1–3) (2012) 115–123.
[40] G. Cheng, L. Sun, L. Jiao, L. Peng, Z. Lei, Y. Wang, J. Lin, Adsorption of methylene blue by residue biochar from copyrolysis of dewatered sewage sludge and pine sawdust, Desalin. Water Treat. (2013). doi: 10.1080/19443994.2013.773265.
[41] W. Tsai, H. Chen, K. Kuo, C. Lai, T. Su, Y. Chang, J. Yang, The adsorption of methylene blue from aqueous solution using waste aquacultural shell powders, J. Environ. Eng. Manage. 19(3) (2009) 165–172.